NO reduction by CO over automotive exhaust gas catalysts in the presence of O_2

J.M.A. Harmsen, J.H.B.J. Hoebink * and J.C. Schouten

Laboratory of Chemical Reactor Engineering, Schuit Institute of Catalysis, Eindhoven University of Technology, PO Box 513, 5600 MB Eindhoven, The Netherlands
E-mail: J.H.B.J.Hoebink@tue.nl

Received 11 July 2000; accepted 31 October 2000

The reduction of NO by CO in absence and presence of O_2 has been investigated by transient experiments at automotive cold-start conditions over Pt/Rh/CeO_2/γ-Al_2O_3, and derived model catalysts. A high-resolution magnetic sector mass spectrometer was used for distinguishing CO/N_2 and CO_2/N_2O. Mechanistic comparisons are made between the catalyst formulations. A kinetic scheme of elementary reaction steps is proposed, which highlights the various contributions of the catalyst constituents.

KEY WORDS: NO reduction; automotive exhaust; platinum; rhodium; ceria; lean; elementary steps; modelling

1. Introduction

Nowadays, removal of harmful components in an automotive exhaust is commonly achieved by the application of a so-called three-way catalytic converter. During the cold-start period, i.e., before the light-off of the monolith, the low temperature of the catalytic surface causes too slow reaction kinetics to achieve a full conversion of all pollutants, resulting in a major contribution to pollution. Therefore, a detailed insight in the relevant reaction mechanisms and kinetics at cold-start conditions could assist in optimisation of the catalytic converter and/or the catalytic formulation, as well as in the development of new control strategies [1].

Especially NO reduction to N_2 has proven to be a large problem, because of a low conversion of NO in the exhaust under lean conditions. This is also a main drawback of the application of lean-burn and diesel engines, which produce exhaust gases with high oxygen concentrations.

The mechanism of the catalytic reduction of NO for automotive purposes has been widely studied. Notably NO reduction by hydrocarbons draws a lot of attention nowadays for its potential application under net oxidising conditions. NO reduction by CO under excess oxygen, however, is still not well understood from a viewpoint of elementary step kinetics, which is an important item since automotive operating conditions are dynamic while ceria is present in automotive catalysts as an oxygen storage component. Therefore, the NO reduction by CO is studied in this paper with transient kinetic methods via cycling of the reactor feed composition.

As noble metals Pt, Rh, Ru, Pd, Ir and alloys on alumina, ceria and ceria/alumina have been investigated [2]. Rh-containing catalysts were found to achieve higher NO conversion than other noble metals [3,4].

* To whom correspondence should be addressed.

The type of support material was found to have a small influence on the kinetics of the NO reduction [5]. An exception concerns the presence of ceria. Ceria can take up the oxygen from dissociating NO on the noble metal [5,6], although this is also explained by an oxygen spill-over from the noble metal to the ceria surface [7]. Furthermore, it was found that NO is able to adsorb onto reduced ceria in combination with oxygen transfer from ceria to the noble metal [8–10]. Maunula et al. [11] investigated the reduction of NO by hydrogen over several catalysts with transient response techniques. They found that ceria-containing catalysts have a higher activity and a higher surface capacity than catalysts without ceria. Trovarelli [9] mentions that NO adsorbs onto ceria which promotes NO desorption as N_2 at much lower temperatures than ceria-free samples.

Generally, three different mechanisms have been proposed in literature. The most used mechanism [4,12–16] involves reversible associative adsorption of both CO and NO on vacant noble metal sites. Subsequent NO dissociation requires another vacant noble metal site. The nitrogen adatoms may recombine to form N_2, or react with another adsorbed NO to form either gaseous N_2O or gaseous N_2, leaving an oxygen adatom on the surface. Adsorbed CO reacts with oxygen adatoms to give gaseous CO_2. According to Permana et al. [16], this mechanism is not altered when oxygen is present in the gas phase. Leclerq et al. [17] proposed a similar mechanism to explain the reduction of NO by CO in the presence of O_2. Generally it is concluded that O_2 adsorption inhibits the NO reduction, but at very low oxygen concentrations oxygen may create additional vacant sites, leading to an enhancement of the NO dissociation.

In an alternative mechanism [18–20], the dissociation of adsorbed NO does not require a vacant noble metal site, but is assisted by adsorbed CO, yielding gaseous CO_2, a nitro-

gen adatom and a vacant site. The influence of oxygen was not considered in that context.

Another mechanism [21–23] proposes two adsorbed NO molecules, which react together to form either gaseous nitrogen or N_2O and oxygen adatoms. Also in this case, no vacant sites for NO dissociation are required and this mechanism is said not to be altered by the presence of gaseous oxygen [22].

This paper provides new mechanistic insight into the contributions of the separate components of a commercial $Pt/Rh/CeO_2/\gamma\text{-}Al_2O_3$ three-way catalyst in terms of elementary steps, e.g., the interactions of NO with ceria. A unique perspective is given, by comparing transient experiments over the $Pt/Rh/CeO_2/\gamma\text{-}Al_2O_3$ catalyst with experiments using the model formulations $Pt/\gamma\text{-}Al_2O_3$ and $Pt/Rh/\gamma\text{-}Al_2O_3$, and their respective carriers $\gamma\text{-}Al_2O_3$ and $CeO_2/\gamma\text{-}Al_2O_3$. The introduction of a high-resolution mass spectrometer in this type of research allows measuring all relevant compounds, including CO and N_2, separately.

2. Experimental

The experimental set-up, used for the transient reduction of nitric oxide by carbon monoxide via cyclic feeding, has already been described in detail [24–27]. By means of magnetic valves, two gas feeds, each having a different composition, and kept separated up to the catalyst bed via release valves, can be alternated over the fixed-bed reactor with an adjustable frequency up to 10 Hz. One feed contains the rich compound CO, the other the lean components NO and O_2. Typical Otto engine exhaust gas concentrations were applied with He as a diluent. The total gas flow of each feed was always equal to 5.6 mmol/s. The total pressure was kept constant at 110 kPa.

Compared to earlier reported experiments with this set-up, the gas analysis was changed. The transients in the gas composition were monitored in real time just above and below the catalyst bed by an on-line magnetic sector mass spectrometer (Jeol JMS-GCmate) at a resolution of 5000 (20% cut), enabling separation of the isobaric masses of CO ($m/e = 27.9949$) and N_2 ($m/e = 28.0062$) on the one hand, and CO_2 ($m/e = 43.9898$) and N_2O ($m/e = 44.0011$) on the other hand. As far as known, this is the first application of a high-resolution mass spectrometer for this type of research. Mass spectrometry analysis was carried out in selected ion monitoring (SIM) mode with a sampling frequency of 25 Hz on N_2, CO, NO, O_2, CO_2, N_2O, and NO_2. All experiments were performed in an isothermal reactor, as observed from thermocouple measurements. An example of measured inlet signals of CO, NO, and O_2 versus time can be seen in figure 1. The signals approach a perfect block form. The reactor residence time is very short (approximately 10 ms) compared to the time scale of the experiments.

The catalysts and carriers were provided by Degussa Metals Catalytic Cerdec A.G., d**mc**^{2}. The catalysts contain 0.398 wt% Pt, 0.080 wt% Rh (if present), and 28 wt% ceria (if present), with $\gamma\text{-}Al_2O_3$ as support. The noble metal capacity equals 8.0 mmol/kg for the Pt catalyst, 12.1 mmol/kg for the Pt/Rh catalyst, and 18.0 mmol/kg for the ceria-containing catalyst. These capacities were determined by CO chemisorption, using stoichiometries of 1 CO per Pt and 2 CO molecules per Rh atom [24]. The reactor contained typically 0.9 g of catalyst or carrier and 1.4 g of inert $\alpha\text{-}Al_2O_3$ (0.15–0.21 mm) for dilution. The catalysts and carriers were pre-treated at 773 K with oxygen in helium during 1 h, followed by reduction with hydrogen in helium for 2 h. More details on this procedure were reported elsewhere [24, 26]. All experiments were carried out under conditions for intrinsic chemical kinetics, when judged with well-known criteria that were developed for steady state kinetic research. For the majority of data, the intrinsicity is not affected by cycling of the feed [25], although this cannot be guaranteed

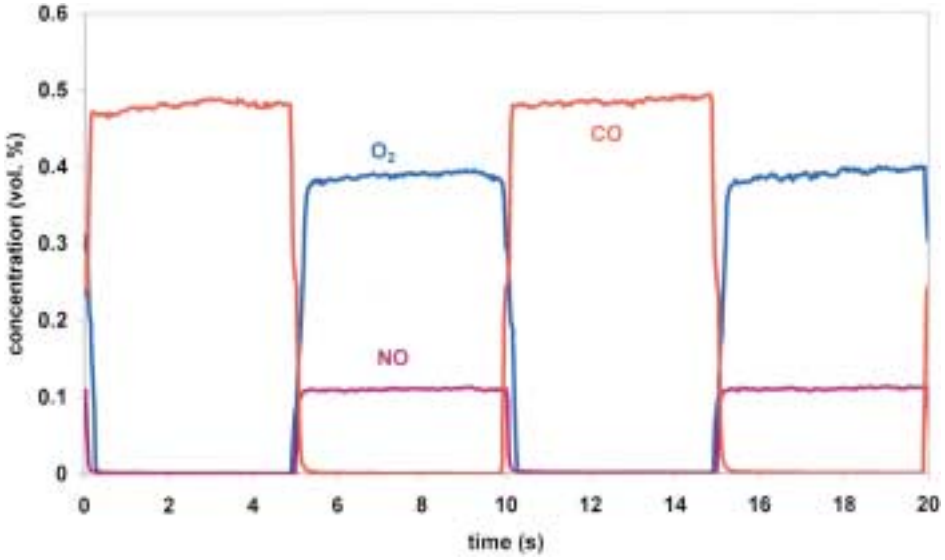

Figure 1. Reactor inlet concentrations versus time, alternating 0.5 vol% CO in He with 0.1 vol% NO and 0.4 vol% O_2 in He at 1/10 Hz.

Table 1
Range of experimental conditions.

p_{TOT}	110 kPa
p^0_{CO}	0.0–0.55 kPa
p^0_{oxygen}	0.35–1.05 kPa
p^0_{NO}	0.0–0.10 kPa
f	0.1–0.05 Hz
T	523–548 K

very shortly after switching from one feed to the other. The range of the experimental conditions is depicted in table 1.

3. Results and discussion

In this section, the experimental results are presented and discussed in order of increasing catalyst complexity. First, the influence of the separate carriers is shown, where after an elementary step model for the Pt/γ-Al_2O_3 is presented, based on the experimental results. Subsequently, the differences between this catalyst and the Pt/Rh/γ-Al_2O_3 and Pt/Rh/CeO_2/γ-Al_2O_3 catalysts are presented. All experiments shown were performed at a reactor temperature of 548 K. The oxidation of carbon monoxide is assumed to proceed as described by the kinetic models of Nibbelke et al. [26] for the ceria-containing catalyst and Hoebink et al. [25] for the non-ceria-containing catalysts.

3.1. The carriers: γ-Al_2O_3 and CeO_2/γ-Al_2O_3

No reaction or adsorption of NO, CO, and O_2 on pure γ-Al_2O_3 was observed. The carrier can therefore be assumed as inert. In a previous study, it was found that CO_2 can reversibly adsorb onto the carrier [25,26].

The ceria/alumina carrier, containing 28 wt% ceria, was investigated for its behaviour towards NO. Starting from completely reduced ceria, it was found that NO is able to adsorb and desorb onto the ceria surface. Figure 2 shows reactor outlet concentrations of NO versus time when 0.1 vol% NO in He is alternated with pure He at 1/20 Hz. The delay in reaching the 0.1% inlet level (interval 20–30 s) corresponds with NO adsorption, while the tail approaching zero (t = 30–40 s) concerns NO desorption. When adsorption on ceria sites is assumed, it can be described as

$$NO_{(g)} + s \rightleftharpoons NOs \quad (1)$$

In this text, the forward step will be referred to as step f, while the backward step is alluded to as step b. Here "s" denotes vacant sites on the ceria. A subsequent experiment with NO and CO in alternating feeds did not yield significantly reaction products, thus excluding chemical reactions on the surface. Apparently ceria is unable to dissociate NO at 548 K. Also, no significant adsorption and desorption of CO was observed.

When oxygen is fed to ceria after the standard pretreatment procedure and exposure to NO, oxygen does not adsorb, meaning that NO blocks reduced ceria sites. Furthermore, after hours of exposure of ceria to NO, a very slow desorption of the latter into a helium flow can be observed even after hours of time-on-stream. This indicates that NO can diffuse into the reduced ceria lattice, as is already known for oxygen. As this process takes place on a time scale much longer than the time scale of feed alterations during the transient experiments, NO bulk diffusion was discarded with respect to this type of experiments.

After reducing the ceria again for 3 h with 5% H_2 in He at 773 K, the oxygen ability to adsorb onto ceria returned. When CO is fed to oxidised ceria, small amounts of CO_2 are found. Significant CO conversion could, however, not be detected.

When, after long-time exposure to oxygen, NO and He are alternated again over the catalyst carrier, exactly the

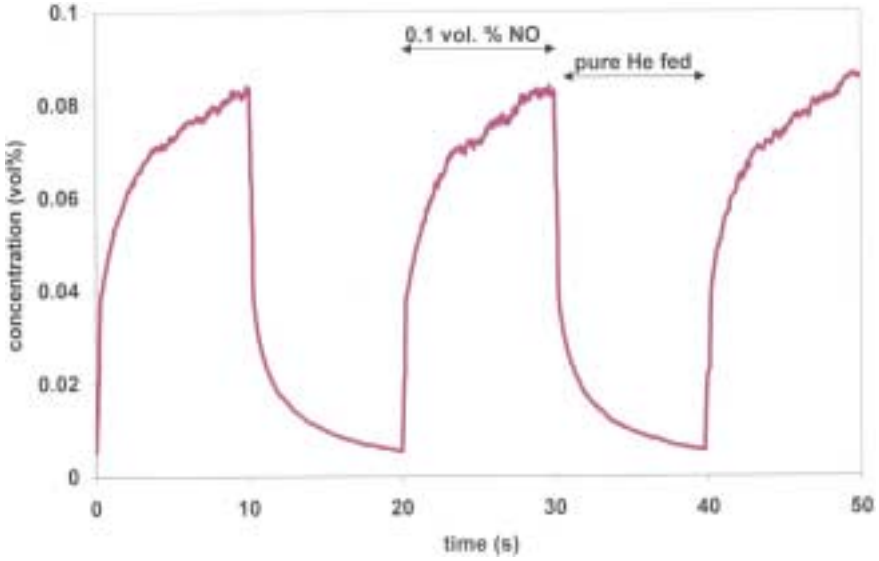

Figure 2. Reactor outlet concentrations of NO, when alternating 0.1 vol% NO in He with a pure He flow over CeO_2/γ-Al_2O_3 at 548 K. The oxidation state of ceria does not matter.

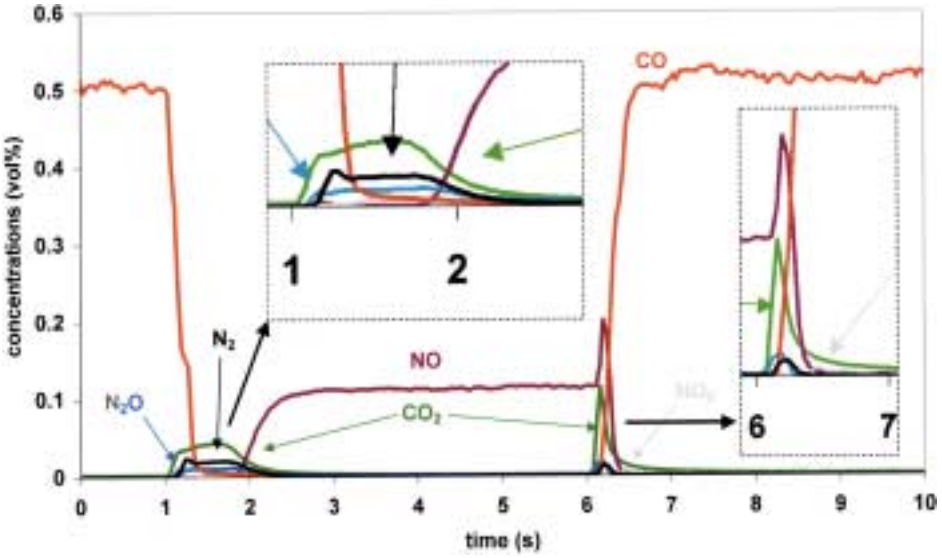

Figure 3. Reactor outlet concentrations versus time, alternating 0.5 vol% CO in He with 0.1 vol% NO in He at 1/10 Hz, at 548 K over Pt/γ-Al_2O_3.

same adsorption and desorption behaviour is found as for the reduced ceria, see figure 2. This means that NO adsorbs on both reduced and oxidised ceria with the same rate. This requires additional elementary steps:

$$NO_{(g)} + Os \rightleftharpoons NO_2s \tag{2}$$

Since, independent of the oxidation state of the ceria, the same amount of NO adsorbs or desorbs, it seems reasonable to assume that the same locations on the catalyst surface are involved. As no gaseous NO_2 was observed during the experiment, it cannot be said whether actually NO_2 is formed on the ceria, or both NO and O are co-adsorbed on the same site.

3.2. The Pt/γ-Al_2O_3 catalyst

Figure 3 shows the results of an experiment where 0.5 vol% CO at the reactor inlet was alternated with 0.1 vol% NO with a frequency of 1/10 Hz. At the end of the CO half-cycle ($t = 1.0$ s) the noble metal surface is assumed to be fully covered by CO. Immediately after the switch to the NO feed has been made, N_2O, CO_2, and N_2 are detected at the end of the reactor. NO remains fully adsorbed by the reactor for approximately 0.3 s. At this temperature CO slowly desorbs, leaving vacant sites onto which NO can adsorb:

$$NO_{(g)} + * \rightleftharpoons NO* \tag{3}$$

Vacant sites on the noble metal are here written as "$*$". The production of N_2O requires the dissociation of NO, which involves extra vacant sites:

$$NO* + * \rightarrow N* + O* \tag{4}$$

N_2O is then formed by

$$NO* + N* \rightleftharpoons N_2O* + * \tag{5}$$

and subsequent desorption:

$$N_2O* \rightleftharpoons N_2O_{(g)} + * \tag{6}$$

Actually, the sorption of N_2O is reversible, as will be shown later. The oxygen adatoms from the dissociating NO will be rapidly converted to CO_2, which was believed to desorb instantaneously [26].

The immediate formation of N_2O together with CO_2 indicates that both N_2O formation (step 5) and desorption (step 6f) are fast under the conditions at that specific time.

Nitrogen can be produced in two different ways, where the first is known to be more important at low temperatures [12,22]:

$$N_2O* \rightarrow N_{2(g)} + O* \tag{7}$$

$$N* + N* \rightarrow N_2 + 2* \tag{8}$$

As the $N*$ coverage will be very low, immediately after switching, and because N_2O is formed immediately, step 7 is more likely to be of importance than step 8 right after the switch.

Finally, a small amount of NO_2 is observed which gradually increases in time during the NO half cycle. The formation of NO_2 requires oxygen adatoms, which will not be present in large quantities just after the switch, but will accumulate on the catalyst surface when the NO half cycle proceeds. In a separate experiment it was found that NO is able to adsorb immediately on a Pt/γ-Al_2O_3 surface fully covered with oxygen, which justifies the forward step (the backward step will be discussed later):

$$NO_{(g)} + O* \rightleftharpoons NO_2* \tag{9}$$

$$NO_2* \rightleftharpoons NO_{2(g)} + * \tag{10}$$

The data do not provide evidence for NO_2 adsorption as its concentration was quite low in all considered experiments.

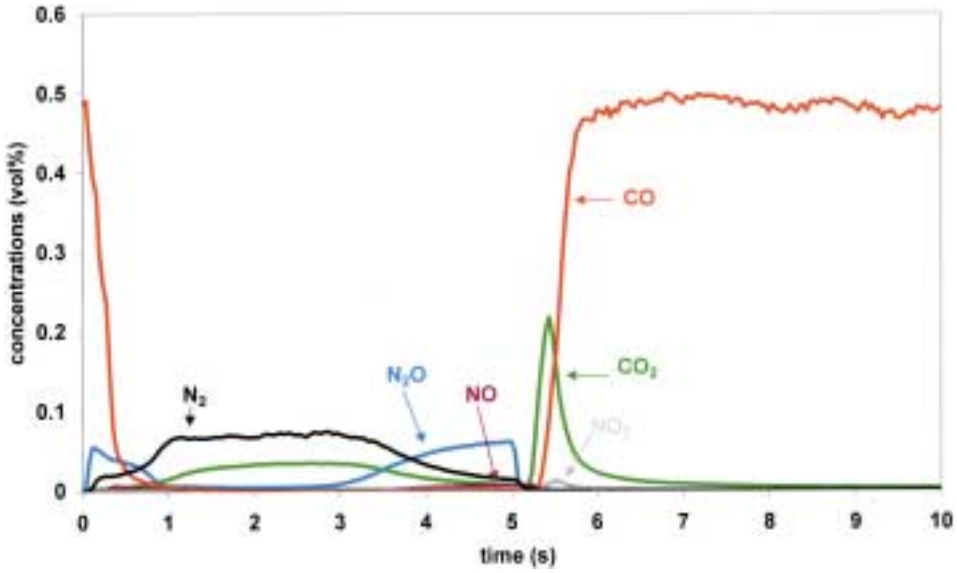

Figure 4. Reactor outlet concentrations versus time, alternating 0.5 vol% CO in He with 0.1 vol% N_2O in He at 1/10 Hz, at 548 K over Pt/γ-Al_2O_3.

After the switch to the lean feed, adsorbed CO on the noble metal surface is gradually exhausted, and replaced by oxygen adatoms and N-containing species. This will lead to a decreasing number of vacant sites, slowing down especially the dissociation of NO (step 4) and the adsorption of NO (step 3f). Therefore, all reactions will gradually stop and the NO concentration will reach its inlet level.

Immediately after the switch from the NO feed to the CO feed is made, strong desorption of NO from the noble metal surface takes place, even to such an extent that the NO concentration temporarily exceeds its inlet level. Such phenomena have been seen before for Ru/SiO_2 and for Pt at 300 K [28,29]. Apparently, NO desorption is a very fast process, which can occur via steps 3b and 9b. Re-adsorption of NO will then be prevented because of the faster adsorption of gaseous CO, which could be seen as a type of cross desorption. A role of adsorbed NO_2 in this process cannot be excluded, as will become clear later. Simultaneously, N_2O, N_2 and CO_2 are produced. This indicates that vacant sites arise on the noble metal surface, enabling dissociation of NO, leading to the mentioned products as described before. The CO_2 production could be ascribed to reaction between adsorbed CO and oxygen adatoms, or between gaseous CO and oxygen adatoms [25]. A very low coverage of oxygen adatoms leads to a very low amount of gaseous NO_2.

Figure 4 shows the results of an experiment, similar to the one in figure 3, except for the fact that N_2O has been fed in the lean half cycle, instead of NO. It can be seen that adsorption of N_2O is (step 6b) a slower process than the adsorption of NO (step 3f), as the former adsorbs only in part on the noble metal surface immediately after the switch from CO to N_2O ($t = 0$ s). The N_2O adsorption is accompanied by N_2 production, which points to step 7.

After the initial break-through of the N_2O signal, N_2O adsorbs almost completely, when sufficient sites have become available through CO desorption and reaction to N_2 (step 7). The latter reaction yields oxygen adatoms, which will react with adsorbed CO. The slow start of the CO_2 production is remarkable, as O adatoms should be available from N_2O decomposition. It is possible that some N_2O decomposes into NO (step 5b), which can desorb (step 3b) and then cover the oxygen adatoms (step 9f).

When comparing figures 3 and 4, it can be seen that the reduction of N_2O (figure 4) yields much more N_2 than the reduction of NO (figure 3). There are two reasons: (1) the stoichiometry leads to twice as much N_2 in the case of N_2O compared to the reduction of NO, and (2) NO reduction requires vacant sites for the dissociation of NO (step 4), while vacant sites are not required for N_2O decomposition (step 7). This means that in the N_2O case the reactions will stop only when the surface becomes largely occupied with oxygen adatoms. The latter apparently occurs near the end of the lean half-cycle, when N_2 and CO_2 production declines, and the N_2O concentration rises to the inlet level. A small amount of NO is observed as well, indicating that step 5 is reversible. The high O coverage is also resembled by the larger CO_2 peak, when switching from the N_2O half cycle to the CO half cycle ($t = 5.3$ s). It is remarkable that in the N_2O experiments similar quantities of NO_2 were measured as in the NO experiments. This also indicates that some N_2O decomposes into NO, which may adsorb on O adatoms and desorb as NO_2.

The outlet concentrations versus time of an experiment where $NO + O_2$ is alternated with CO can be seen in figure 5. When compared with the same experiment in the absence of oxygen (figure 3), the NO signal shows two major differences: much less adsorption takes place at the beginning of the NO half cycle showing even a small breakthrough peak, and the desorption behaviour after the switch to the CO half cycle is completely different. The difference in adsorption can be explained by the relatively fast adsorption and reaction of oxygen. The CO_2 peak, when O_2 is

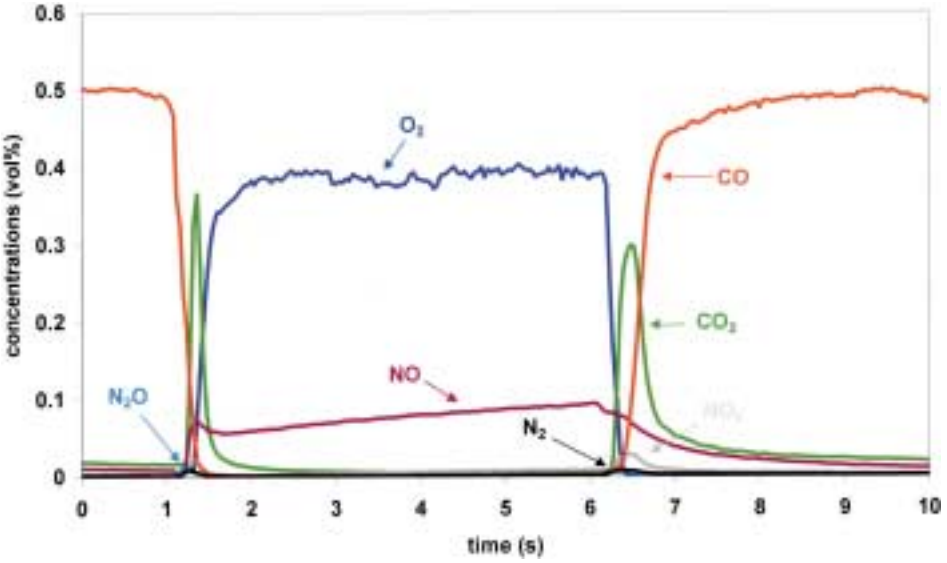

Figure 5. Reactor outlet concentrations versus time, alternating 0.5 vol% CO in He with 0.1 vol% NO and 0.4 vol% O_2 in He at 1/10 Hz, at 548 K over Pt/γ-Al_2O_3.

fed, is high and sharp, indicating a very fast oxidation of adsorbed CO by adsorbing O_2. This means that the surface will quickly be dominated by oxygen adatoms onto which NO is apparently able to adsorb quite slowly through step 9f. NO adsorbs immediately on both vacant sites (only few are available as can be seen from the small N_2 and N_2O production) and O adatoms, but both reaction rates are too slow to reach a full NO conversion. NO adsorption on O$*$ leads to NO_2 desorption, as seen from the NO_2 gas phase concentration, which slowly increases in time. The NO adsorption proceeds quite long, however, because the NO signal very slowly approaches its inlet level. NO_2 (step 10f) and NO (step 9b) desorption seems rather slow as appears from the tailing of the NO_2, NO, and CO_2 signals.

After the switch to the CO half cycle, oxygen adatoms are available for reaction with CO to CO_2 either directly or by desorption of NO from adsorbed NO_2. The relatively large NO_2 peak ($t = 6.5$ s) indicates vacant sites become available as well. The catalyst surface is mostly covered with NO_2 at the end of the lean half cycle. This is supported by the long tail in the CO_2 signal, which emanates from the oxygen adatoms formed by a slow NO_2 decomposition. The high and immediate peak in the CO_2 signal may indicate that CO reacts via both Langmuir–Hinselwood and Eley–Rideal type of steps [25]. At both switching moments, the production of N_2 and N_2O is very low, because of the low fraction of vacant sites on the noble metal, which are required for the dissociation of NO (step 4). The NO_2 responses at the second half of both half cycles follow the gas phase concentration of NO in either a slow decrease (CO half cycle) or a slow increase (NO half cycle).

3.3. The Pt/Rh/γ-Al_2O_3 catalyst

The influence of Rh in the catalyst is derived from a comparison of transient experiments on a Pt/Rh/γ-Al_2O_3 catalyst and on the Pt/γ-Al_2O_3 catalyst, described before.

Figure 6 shows an experiment with alternating 0.5 vol% CO in He and 0.1 vol% NO in He. This figure compares with figure 3 on the Pt catalyst. The major difference is the larger conversion of all compounds on the Pt/Rh catalyst. The CO_2 peak at the switch from the CO feed to the NO feed ($t = 1.3$ s) has a much larger area. This area is almost fully determined by the amount of CO, adsorbed on the catalyst just before this switch. The larger area indicates that the Pt/Rh catalyst simply contains more active noble metal sites than the Pt catalyst. This already explains the major differences between the two catalysts. There are, however, some other dissimilarities.

Immediately after the switch from the CO feed to the NO feed ($t = 1.3$ s) more N_2 and less gaseous N_2O is produced than on the Pt catalyst, which indicates that the decomposition of N_2O is faster on the Pt/Rh catalyst. The enhanced dissociation of NO, caused by the presence of Rh, can also be seen from the quite large N_2 peak at the switch from NO to CO ($t = 6.0$ s). The NO signal misses its sharp desorption peak, which is present in the Pt catalyst experiment. Clearly, the dissociation/desorption ratio of NO is more favourable when Rh is present.

While the Pt catalyst produces N_2O two times per period, the N_2O signal from the Pt/Rh catalyst has three maxima. At the end of the CO half cycle, the noble metal surface is more or less fully covered with CO. After the switch to NO has been made, some CO will desorb, and NO can adsorb (step 3) and partly dissociate (step 4) on the vacant sites. This will give N$*$ next to NO$*$ on the noble metal surface leading to the first N_2O maximum at $t = 1.3$ s (steps 5 and 6). The proceeding reactions produce extra vacant sites, which enhances the dissociation rate of NO and decreases the N_2O production. When surface CO gets depleted, CO_2 formation decreases, so it will become more difficult to re-

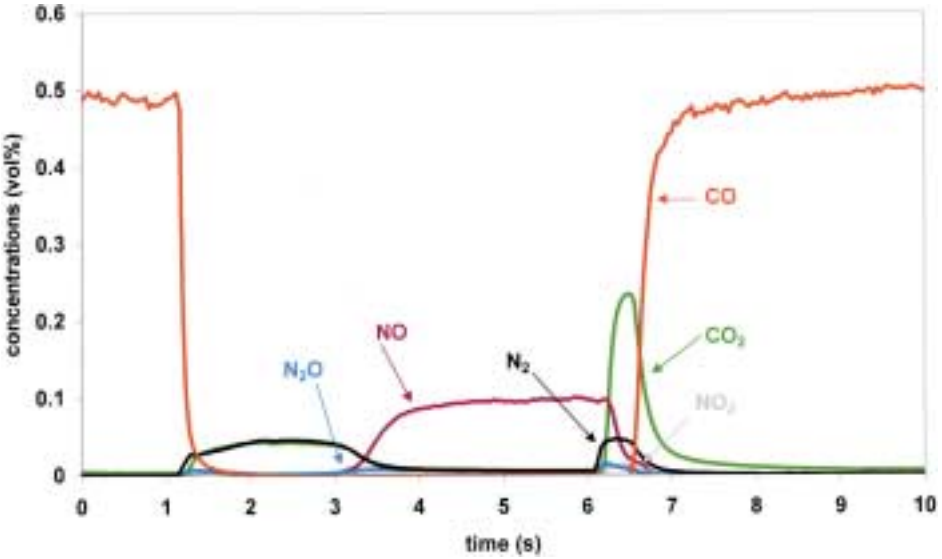

Figure 6. Reactor outlet concentrations versus time, alternating 0.5 vol% CO in He with 0.1 vol% NO in He at 1/10 Hz, at 548 K over Pt/Rh/γ-Al_2O_3.

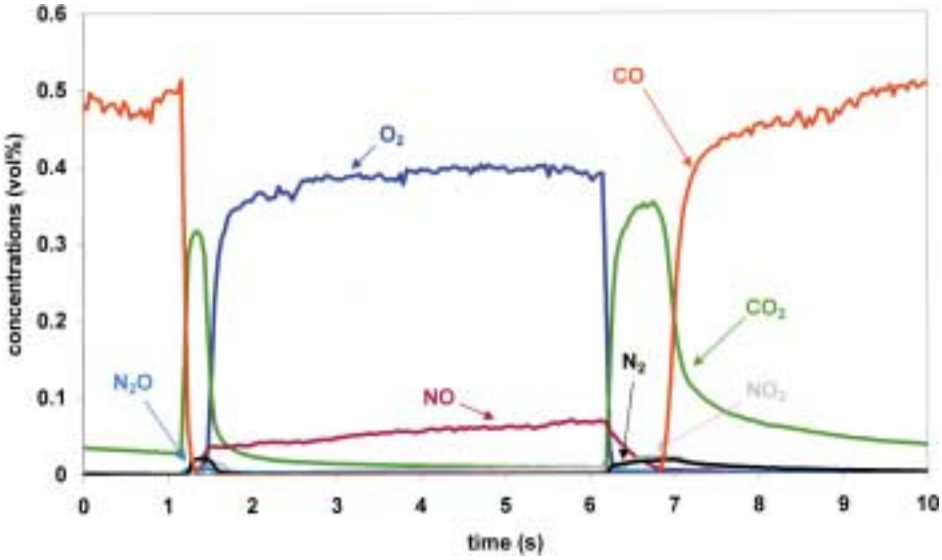

Figure 7. Reactor outlet concentrations versus time, alternating 0.5 vol% CO in He with 0.1 vol% NO and 0.4 vol% O_2 in He at 1/10 Hz, at 548 K over Pt/Rh/γ-Al_2O_3.

move O$*$ from the surface. Due to fewer vacant sites, not all NO can dissociate anymore, and the resulting N adatoms next to molecular adsorbed NO will form N_2O for the second time until the end of the NO half cycle. Only when the switch to the CO feed is made, are vacant sites created again to invoke N_2O production.

Also for the Pt/Rh catalyst the influence of the presence of oxygen is large. Figure 7 shows the results of a transient experiment where CO is alternated with a mixture of NO and O_2. This figure is compared to figure 5 for the Pt catalyst. Especially the conversion of CO and O_2 is much higher over the Pt/Rh catalyst, resulting in larger CO_2 peaks. Also more NO is converted to N_2, as was also seen in the experiments without O_2. NO adsorption is more pronounced and there is less desorption. These aspects can again be ascribed to the above mentioned changes in number of sites, leading to higher conversions of all compounds. Also reaction rates for most steps involving NO will be higher on the Pt/Rh catalyst compared to the Pt catalyst. Summarising the effect of Rh addition to a Pt catalyst, it can be said that the mechanism is not altered, but that the rates of especially the following steps are higher: NO dissociation (step 3), N_2O decomposition (step 7), NO_2 formation (step 9f). This is an important conclusion for kinetic modelling, as it appears that no distinction has to be made between Pt and Rh sites.

3.4. The Pt/Rh/CeO_2/γ-Al_2O_3 catalyst

The experimental results from the previous section are compared with similar transient experiments over a commercially available Pt/Rh/CeO_2/γ-Al_2O_3 catalyst. As this catalyst contains ceria, steps 1 and 2 apply here as well. Figure 8

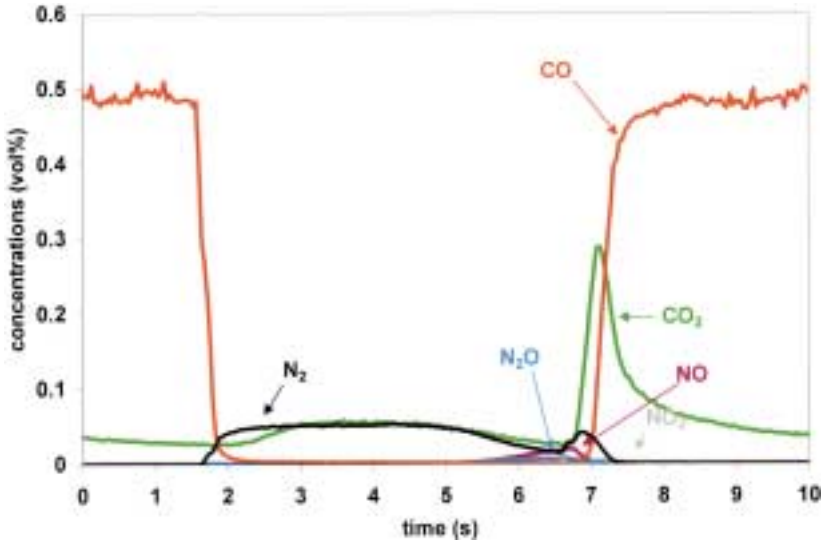

Figure 8. Reactor outlet concentrations versus time, alternating 0.5 vol% CO in He with 0.1 vol% NO in He at 1/10 Hz, at 548 K over Pt/Rh/CeO_2/γ-Al_2O_3.

shows the results of an NO reduction experiment in the absence of O_2, which is comparable with the experiment from figure 6 over the Pt/Rh catalyst. The major differences between the two experiments are the amounts of N_2 and CO_2 produced: the ceria-containing catalyst produces more than twice as much of both products. As was mentioned before, the production of N_2 during the NO half cycle will stop when NO dissociation is hindered by absence of vacant sites because of accumulation of oxygen adatoms on the noble metal surface. The fact that this moment is strongly delayed for the ceria catalyst, indicates that ceria is able to take oxygen from dissociated NO. Two possible pathways for this process are known from literature: oxygen adatoms could spill over to the ceria surface [7], or a type of bifunctional dissociation of NO adsorbed on the noble metal could take place [5,6]:

$$\mathrm{NO}* + \mathrm{s} \rightarrow \mathrm{N}* + \mathrm{Os} \qquad (11)$$

As can be seen in figure 8 ($t = 2$–6 s), the NO conversion is complete for almost the entire half cycle, and also the N_2O production is very low. Under these conditions the dissociation of NO is quite fast, so the fractional surface coverage of NO is expected to be very low. The main path for N_2 formation is therefore likely to be the recombination of two N adatoms into N_2 (step 8). Only near the end of the NO half cycle, the N_2O and NO concentrations start to rise, indicating a significant decrease in the fraction of vacant sites. The absence of a large amount of oxygen on the noble metal also leads to a very low amount of NO_2 produced. The increased oxygen storage can very well be seen from the large CO_2 peak after the switch from the NO to the CO half cycle. Its increased area, compared with the experiment over the Pt/Rh catalyst, is directly related with the larger oxygen storage capacity of the ceria catalyst. Besides the presence of ceria, also a larger noble metal dispersion is a partial explanation for larger storage capacities of the catalyst.

As hardly any NO is present on the catalyst, no desorption is detected after the switch to the CO feed. It is remarkable that the amount of CO_2 produced in the NO half cycle over the ceria-containing catalyst is more than the corresponding amount of CO_2 produced in the NO half cycle over the Pt/Rh catalyst. Principally, the amount of CO_2 produced after the switch to the NO feed, is solely determined by the amount of CO on the catalyst just before the switch is made. Apparently, the ceria-containing catalyst can store more CO than the Pt/Rh catalyst. The higher noble metal capacity can probably only partly explain this difference. Other explanations could be reversible CO spill-over from the noble metal to the ceria, or differences in CO adsorption/desorption equilibria leading to higher surface coverages on the ceria catalyst compared to the Pt/Rh catalyst during the rich half cycle.

The transient reduction of NO by CO in the presence of O_2 over the commercial Pt/Rh/CeO_2/γ-Al_2O_3 catalyst can be seen in figure 9. Compared with figure 7 for the Pt/Rh catalyst, it can be seen that ceria has a large influence on all conversions. When ceria is present much more NO adsorbs, but significantly less than in the absence of oxygen (figure 8). Combined with the fact that much less N_2 is produced, it can be concluded again that the dissociation of NO is largely inhibited by the oxygen on the noble metal. Oxygen inhibition does not hinder NO adsorption on ceria, which NO is released after the switch to the CO feed is made. The desorption peak is likely a combination of desorption from the noble metal, probably from NO_2* decomposition because of the relatively slow desorption, and desorption of NO from ceria. The N_2O signals follow the N_2 signals, indicating that under these conditions the decomposition of N_2O is the most important path for N_2 formation.

Both CO_2 peaks are larger for the commercial catalyst than for the Pt/Rh catalyst. As before, the CO_2 peak in the CO half cycle can be explained by the presence of oxygen on ceria, which can oxidise CO on the noble metal via the bifunctional path [26]. This path is hindered by NO, adsorbed onto ceria oxygen (step 2) explaining the long CO_2 tail at

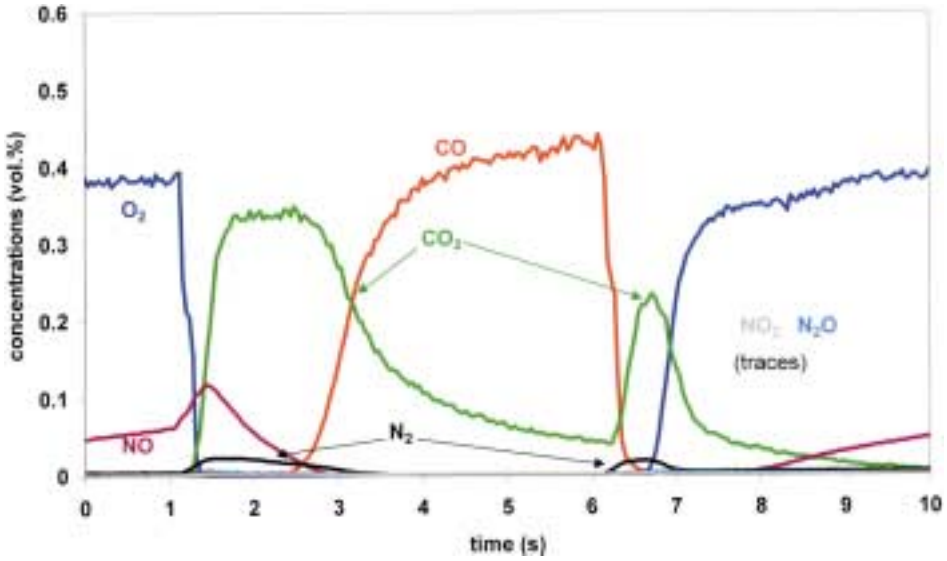

Figure 9. Reactor outlet concentrations versus time, alternating 0.5 vol% CO in He with 0.1 vol% NO and 0.4 vol% O_2 in He at 1/10 Hz, at 548 K over Pt/Rh/CeO_2/γ-Al_2O_3.

Table 2
Elementary step model for the transient NO reduction by CO in the presence of O_2 over a Pt/Rh/CeO_2/γ-Al_2O_3 three-way catalyst.[a]

Step No.	Elementary reaction step
1	$NO_{(g)} + s \rightleftharpoons NOs$
2	$NO_{(g)} + Os \rightleftharpoons NO_2s$
3	$NO_{(g)} + * \rightleftharpoons NO*$
4	$NO* + * \rightarrow N* + O*$
5	$NO* + N* \rightleftharpoons N_2O* + *$
6	$N_2O* \rightleftharpoons N_2O_{(g)} + *$
7	$N_2O* \rightarrow N_{2(g)} + O*$
8	$N* + N* \rightarrow N_2 + 2*$
9	$NO_{(g)} + O* \rightleftharpoons NO_2*$
10	$NO_2* \rightleftharpoons NO_{2(g)} + *$
11	$NO* + s \rightarrow N* + Os$

[a] The steps for CO oxidation were reported in [26].

the last part of the half cycle. The increased CO_2 production after the switch to the NO + O_2 half cycle can again only be explained by the presence of CO on the ceria caused by spill-over from the noble metal during the CO half cycle.

A complete model for NO reduction by CO under net oxidising conditions over a Pt/Rh/CeO_2/γ-Al_2O_3 catalyst is summarised in table 2, which results from adding additional steps for bifunctional reactions and reactions on ceria to the elementary step model, proposed for the noble metal catalyst without ceria.

4. Conclusions

- Various constituents of the commercial Pt/Rh/CeO_2/γ-Al_2O_3 catalyst have been studied separately with respect to the transient reduction of NO by CO in the presence and absence of oxygen.
- The comparison of several model catalyst formulations is a successful approach for understanding complex industrial catalysts.
- The transient experiments provided new mechanistic insights, such as: reversible adsorption of NO on ceria appeared independent of the oxidation state of ceria, indications of bulk diffusion of NO into ceria, ceria cannot dissociate NO, but can store O atoms from NO dissociating on the noble metal.
- Chemisorbed CO does not directly react with chemisorbed NO, but leads to additional desorption of NO through cross-desorption.
- N_2 and N_2O formation only occur after NO dissociation, which is inhibited by the presence of oxygen.
- The main path for N_2 formation proceeds by N_2O decomposition.
- The reduction of gaseous N_2O proceeds slower than the reduction of NO, because of slow N_2O adsorption.
- The presence of Rh in the catalyst accelerates the rate of certain reaction steps, but does not alter the mechanism.
- A high resolution mass spectrometer is a very useful tool for transient experiments, in which isobaric masses occur.

Acknowledgement

Financial support for this research was given by the Dutch Technology Foundation (STW). The authors are grateful to d**mc**^{2} A.G. for providing the catalysts. T.F.A. Pijls and S.T.A. Paalvast are gratefully acknowledged for their contributions.

References

[1] M. Balenovic, A.J.L. Nievergeld, J.H.B.J. Hoebink and A.C.P.M. Backx, SAE-paper 1999–01-3623.
[2] H. Muraki and Y. Fujitani, Ind. Eng. Chem. Prod. Res. Dev. 25 (1986) 419.
[3] V.A. Matyshak, R.A. Gazarov, V.I. Panchishnyi and A.A. Kadushin, Kinet. Katal. 29 (1988) 1206.
[4] P. Granger, J.J. Lecomte, C. Dathy, L. Leclercq and G. Leclercq, J. Catal. 175 (1998) 194.
[5] S.H. Oh and C.C. Eickel, J. Catal. 128 (1991) 526.
[6] R.P. Underwood and A.T. Bell, J. Catal. 111 (1988) 325.
[7] P. Lööf, B. Kasemo, L. Björnkvist, S. Andersson and A. Frestad, Stud. Surf. Sci. Catal. 71 (1991) 253.
[8] H. Cordatos and R. Gorte, J. Catal. 159 (1996) 112.
[9] A. Trovarelli, C. de Leitenburg, M. Boaro and G. Dolcetti, Catal. Today 50 (1999) 353.
[10] A.F. Diwell, R.R. Rajaram, H.A. Shaw and T.J. Truex, Stud. Surf. Sci. Catal. 71 (1990) 139.
[11] T. Maunula, J. Ahola, T. Salmi, H. Haario, M. Härkönnen, M. Luoma and V. Pokjola, Appl. Catal. B 12 (1997) 287.
[12] R.R. Sadhankar and D.T. Lynch, Ind. Eng. Chem. Res. 36 (1997) 4609.
[13] Th. Fink, J. Dath, M.R. Basset, R. Imbihl and G. Ertl, Surf. Sci. 245 (1991) 96.
[14] D. Lorimer and A.T. Bell, J. Catal. 59 (1979) 223.
[15] W. Hecker and A.T. Bell, J. Catal. 84 (1983) 200.
[16] H. Permana, K.Y. Simon Ng, C. Peden, S.J. Schmieg, D.K. Lambert and D.N. Belton, Catal. Lett. 47 (1997) 5.
[17] G. Leclerq, C. Dathy, G. Mabilon and L. Leclerq, Stud. Surf. Sci. Catal. 71 (1991) 181.
[18] R.L. Klein, S. Schwartz and L.D. Schmidt, J. Phys. Chem. 89 (1985) 4908.
[19] B.A. Banse, D.T. Wickham and B.E. Koel, J. Catal. 119 (1989) 238.
[20] J.P. Huinink, Ph.D. Dissertation, Eindhoven University of Technology (1995).
[21] A. Kudo, M. Steinberg, A. Bard, A. Campion, M. Fox, T. Mallouk, S. Webber and J. White, J. Catal. 125 (1990) 565.
[22] L.M. Carballo, T. Hahn and H.-G. Lintz, Appl. Surf. Sci. 40 (1989) 53.
[23] B.K. Cho, B. Shanks and J.E. Bailey, J. Catal. 115 (1989) 486.
[24] M.A.J. Campman, Ph.D. Dissertation, Eindhoven University of Technology (1996).
[25] J.H.B.J. Hoebink, A.J.L. Nievergeld and G.B. Marin, Chem. Eng. Sci. 54 (1999) 4459.
[26] R.H. Nibbelke, A.J.L. Nievergeld, J.H.B.J. Hoebink and G.B. Marin, Appl. Catal. B 19 (1998) 245.
[27] J.M.A. Harmsen, J.H.B.J. Hoebink and J.C. Schouten, Ind. Eng. Chem. Res. 39 (2000) 599.
[28] M.F. Brown and R.D. Gonzales, J. Catal. 47 (1977) 333.
[29] C.M. Comrie and R.M. Lambert, Surf. Sci. 46 (1974) 61.